Chemical Interrogation of Mismatches in DNA−DNA and DNA−RNA Duplexes under Nonstringent Conditions by Selective 2′-Amine Acylation†

Deborah M. John and Kevin M. Weeks*

Department of Chemistry, University of North Carolina, Chapel Hill, North Carolina 27599-3290

Received January 31, 2002

ABSTRACT: 2′-Amine-substituted nucleotides in hybridized duplexes can be chemically tagged in an acylation reaction that is faster for mismatched or flexible nucleotides than for residues constrained by base pairing. Here we explore mismatch and hybridization detection using probe oligodeoxynucleotides containing single 2′-aminocytidine or -uridine nucleotides annealed to DNA or RNA targets under nonstringent conditions, below T_m. Consistent with a mechanism in which 2′-amine acylation is gated by local nucleotide flexibility, we find that efficient acylation is correlated with formation of weaker or fewer hydrogen bonds in base pair mismatches. Using 2′-aminocytidine-containing probes annealed to both DNA and RNA targets, mismatches are reliably detected as rapid selective acylation of the 2′-amine group in two sequence contexts. For probe oligonucleotides containing 2′-aminouridine residues, good discrimination between U-A base pairs and U-G mismatches could be obtained for DNA−DNA but not for DNA−RNA duplexes upon the introduction of a single 2′-O-Me group 5′ to the 2′-amino nucleotide. The 2′-O-Me group introduces a structural perturbation, presumably to a more A-form-like structure, that exaggerates local flexibility at mismatches in DNA strands. Thus, 2′-amine acylation can be used to interrogate all possible mismatches in DNA−DNA duplexes and mismatches involving 2′-amine-substituted cytidine nucleotides in DNA−RNA heteroduplexes. Applications of this chemistry include detecting and chemically proofreading single nucleotide polymorphisms in both DNA and RNA targets and quantifying absolute amounts of RNA.

The ability to selectively tag a nucleotide in a chemical reaction sensitive to the local base pairing environment represents an important step in developing new approaches for detecting single nucleotide polymorphisms and for quantifying RNA levels at single nucleotide resolution. Single nucleotide polymorphisms (SNPs) distinguish, in large measure, one individual from another and are responsible for diverse genetic diseases. Although many different SNP detection methods exist, no single technique is ideal for all types of assays. One criterion for a more universal SNP detection technology would be the ability to interrogate a single nucleotide using a direct method without the requirement to determine discriminatory hybridization conditions. An interrogation chemistry that detects mismatched and locally flexible nucleotides would also be useful for quantifying duplex formation. Thus, development of a robust chemical framework for selectively scoring the base paired state of a nucleotide would also open up new opportunities for quantifying absolute amounts of RNA at single nucleotide resolution.

2′-Amine interrogation exploits our observation that 2′-amine-substituted nucleotides at the site of a base pair mismatch react with succinimidyl esters (Figure 1A) more rapidly than amine substitutions at constrained, base paired nucleotides (*1*). Efficient acylation is not correlated to solvent accessibility at the 2′-ribose position but instead with local nucleotide flexibility. This effect was first demonstrated in structural studies with $tRNA^{Asp}$ in which 2′-amine-substituted nucleotides involved in base paired secondary structures or tertiary interactions were relatively unreactive toward acylation. In contrast, unconstrained nucleotides in loop regions were reactive (*2*). In prior exploratory work, we detected the Factor V Leiden (G1691A) mutation as a reactive C-A mismatch in a duplex comprised of a DNA probe containing a single 2′-amine-substituted cytidine nucleotide hybridized to an oligonucleotide model for the human Factor V gene. To develop a comprehensive picture of the opportunities and limitations of selective 2′-amine interrogation, this work investigates mismatch detection in a different sequence context, using a different 2′-amino nucleotide, and in DNA−RNA heteroduplexes.

We focus on two distinct model systems involving SNPs that contribute to human pathogenesis: the genes for the aryl sulfatase A enzyme (ASA) and the Factor V (FV) clotting factor (Scheme 1). A single A → G transition at position 1049 in the ASA gene causes the encoded asparagine to be read as serine and eliminates an N-glycosylation site on the enzyme (*3*). Significantly, the A → G mutation represents a physiologically relevant opportunity to test discrimination between energetically similar U-A and U-G base pairs in 2′-amine probe−target duplexes. The second system focuses on a common point mutation in the Factor V gene, termed Factor V Leiden. The G → A mutation leads to the replacement of arginine at residue 506 by glutamine and renders the activated form of Factor V resistant to regulated proteolysis by activated protein C (*4*).

† Supported by an NSF Career Award (MCB9984289) to K.M.W.
* Corresponding author. Email: weeks@unc.edu.

10.1021/bi025611d CCC: $22.00
Published on Web 04/30/2002

2′-Amine acylation was able to differentiate all mismatches from a C-G pair at 2′-aminocytidine nucleotides in both DNA−DNA and DNA−RNA duplexes. Discrimination at 2′-amine-substituted uridine nucleotides requires that a single 2′-O-Me group be incorporated 5′ to the 2′-amine group. The adjacent 2′-O-Me nucleotide selectively enhanced 2′-amine acylation reactivity, apparently by enhancing the local flexibility for all base pair mismatches in the context of a DNA−DNA duplex.

EXPERIMENTAL PROCEDURES

Oligonucleotides and Reaction Conditions. DNA and RNA oligonucleotides were synthesized using phosphoramidite chemistry (Dharmacon Research Inc., TriLink BioTechnologies, or the Nucleic Acid Core Facility at the University of North Carolina), purified by denaturing gel electrophoresis (7 M urea, 90 mM Tris−borate, 20% acrylamide), recovered by electroelution, and stored in 10 mM Tris, pH 7.5, 1 mM EDTA. All thermal denaturation and 2′-amine acylation experiments were performed under identical conditions [100 mM Na-Hepes, pH 8.0, 10% dimethyl sulfoxide (DMSO), and 0.5 M NaCl].

Thermodynamic Parameters. Melting experiments were performed at 1 μM in each strand using either an AVIV 17DS spectrophotometer or an AVIV 62DS circular dichroism spectrometer. Melting curves were obtained at a heating rate of 1 °C/min using 1 cm path length cells, monitored at 260 nm. Data obtained using the CD spectrometer were noisier than those obtained with the 17DS spectrometer for which we report larger error limits. For some DNA−DNA and DNA−RNA duplexes, oligonucleotide annealing was monitored by both heating and cooling from 90 °C using the CD spectrometer. Thermodynamic parameters were the same within measurement error, supporting two-state transitions and little or no RNA hydrolysis at pH 8.0. Data were collected every 1 °C, algebraically differentiated, and manually corrected for nonzero baselines. Melting temperature (T_m) and van't Hoff enthalpy (ΔH_{vH}) were obtained by direct fitting of the differential melting curve (*1*, *5*) assuming a bimolecular reaction:

$$\frac{dA_{260}}{dT} = a\frac{f(1-f)}{1+f} \quad (1)$$

where a is a scaling factor, f is the fraction duplex, A_{260} is the absorbance at 260 nm, and T_m and ΔH_{vH} are obtained by substituting into eq 1 the equilibrium expression:

$$f = 1 + (KC_T)^{-1} - \{[1 + (KC_T)^{-1}]^2 - 1\}^{1/2} \quad (2)$$

and the integrated form of the van't Hoff equation:

$$K = K_{T_m} e^{(\Delta H_{vH}/R)(1/T_m - 1/T)} \quad (3)$$

where K is the equilibrium constant, C_T is the total strand concentration, T is absolute temperature, R is the gas constant, and $K_{T_m} = 2 \times 10^6$ M^{-1}. Real duplexes undergo pretransition fraying; therefore, points more than 6−8 K below T_m were excluded during fitting [for representative melting curves, see ref (*1*)]. Although the thermal melting and 2′-amine acylation (see below) experiments are performed at different strand concentrations, the concentration dependence is very small [see eq 3 in (*6*)], and duplex stability under acylation conditions is calculated to be the same, within error, as observed in thermal melting experiments. Thus, the thermal denaturation and chemical acylation experiments performed in this work may be compared without extrapolation. Thermodynamic correction values were obtained from experiments performed in the absence of either 10% DMSO and/or 0.5 M NaCl. ΔG_{35} was calculated from $\Delta G_{35} = -RT \ln K$, where K is given in eq 3.

Selective Acylation. 2′-Amine acylation experiments were performed with excess (0.72 μM for FV or 1 μM for ASA sequences) complementary strand and 1−10 nM ^{32}P-5′-end-labeled probe oligonucleotide in 100 mM Hepes, pH 8.0, and 0.5 M NaCl. Reactions (16 μL, 35 °C) were initiated by addition of a 10× solution of the succinimidyl ester [1× = 75 mM, sulfosuccinimidyl-6-(biotinamido) hexanoate; Pierce Biochemical, Rockford, IL] in DMSO, and aliquots (2 μL) were quenched by addition of 8 μL of stop solution (125 mM DTT in 85% formamide, 45 mM Tris−borate, 50 mM EDTA). Reactions were resolved by denaturing electrophoresis (20% acrylamide, 7 M urea, 90 mM Tris−borate, 4 mM EDTA, with gel dimensions of 0.75 mm × 31 cm × 23 cm at 30 W) and quantified using a Phosphorimager. The succinimidyl ester reacts by 2′-amine acylation and is also inactivated by solvent hydrolysis (*2*). Acylation rates were obtained by fitting acylation profiles to an equation that accounts for these parallel reactions:

$$\text{fraction acylated product} = 1 - \exp\left\{\frac{k_{acyl}}{k_{hydrolysis}}(e^{-k_{hydrolysis}t} - 1)\right\} \quad (4)$$

where k_{acyl} and $k_{hydrolysis}$ are the pseudo-first-order rate constants for 2′-amine acylation and reagent hydrolysis at an ester concentration of 75 mM, respectively. $k_{hydrolysis}$ was found to be equal to 0.025 min^{-1}.

RESULTS

Experimental Design. These studies employed 20-mer DNA probe oligonucleotides incorporating a single nucleotide containing an amine substitution at the 2′-ribose position. Acylation of the 2′-amine group by a succinimidyl ester yields the 2′-amide product (Figure 1A). Acylation occurs selectively at the 2′-amine substitution due to the greater nucleophilicity of the aliphatic amine as compared to nucleic acid base arylamines. The oligodeoxynucleotide probes contain either a 2′-aminocytidine or a 2′-aminouridine nucleotide at position 10 (Figure 1B). The 2′-amine-substituted probe strands are designed to hybridize with DNA or RNA target strands, such that the 2′-amine-substituted nucleotides form a perfect base pair or mismatched base pair with the potential position to be interrogated (denoted as a boldface N in Figure 1B).

We explored the sensitivity of 2′-amine acylation for querying single base changes in two oligonucleotide model systems, each containing a single potential pathogenic SNP. The first sequence corresponds to the human aryl sulfatase A (ASA) gene, in which an A → G transition at position 1049 eliminates a glycosylation site (at Asn350) in the translated protein [Scheme 1, upper panel (*3*)]. A 20-nucleotide target strand was synthesized corresponding to

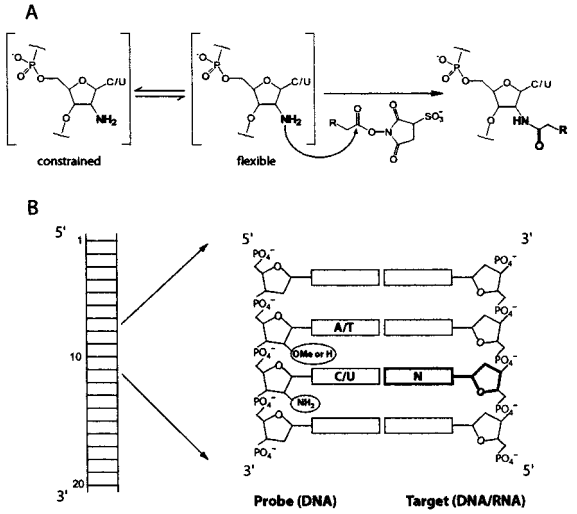

FIGURE 1: 2′-Amine acylation applied to detecting mismatches and nucleic acid hybridization. (A) Reaction of a 2′-amine-substituted nucleotide with an activated ester yields the 2′-amide product and is gated by the underlying local nucleotide structure. The R group for the experiments reported in this work is the biotinamido butyl group. (B) Oligonucleotide model system for detecting potential pathological single nucleotide polymorphisms (SNPs). A DNA probe oligonucleotide containing a single 2′-amine substitution is hybridized to either a DNA or a RNA target strand. The 2′-amino nucleotide will form a perfect or mismatched base pair with the potential SNP, denoted as N. Some probe strands contain a single 2′-O-Me nucleotide 5′ to the 2′-amine-substituted nucleotide.

Scheme 1

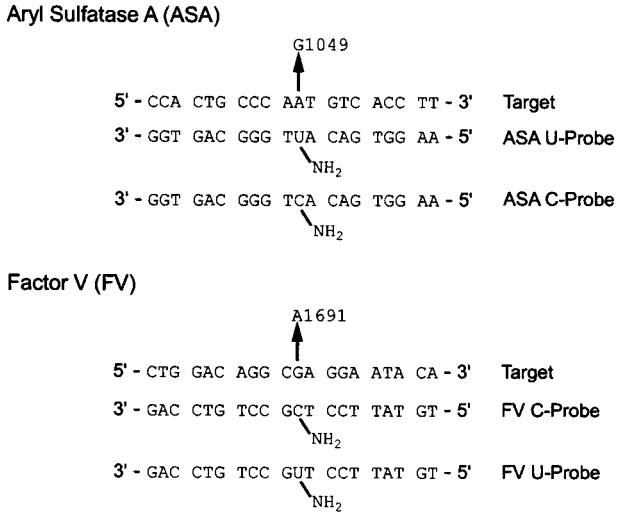

either the wild-type adenine or the mutant guanine base at position 11. The ASA U-probe hybridizes to the target such that the 2′-aminouridine forms a canonical U-A base pair in the case of the wild-type ASA allele or forms a mismatched U-G base pair in the case of the mutant allele (Scheme 1). A mutation detection experiment can equivalently be performed in the reverse format using the ASA C-probe. In this case, the wild-type allele forms a C-A mismatch, and the A1049G SNP forms a C-G base pair (Scheme 1).

Selective 2′-amine acylation was also evaluated for sequences derived from the Factor V (FV) clotting factor gene. The G → A transition at position 1691 is called the Factor V Leiden mutation and leads to disruption of regulated proteolysis of the Factor V protein by activated protein C (*4*). In this case, the wild-type and mutant alleles form a C-G base pair or a C-A mismatch using the FV C-probe, respectively (Scheme 1, lower panel). Again, the reverse experiment is also possible, in which the G1691A mutant allele is scored as a U-A base pair (Scheme 1).

Table 1: Thermodynamic Parameters for 2′-Amine-Substituted DNA−DNA Duplexes[a]

	ASA duplexes					FV duplexes			
	U-probe		2′-OMe U-probe			C-probe		2′-OMe C-probe	
	T_m	ΔG_{35}	T_m	ΔG_{35}		T_m	ΔG_{35}	T_m	ΔG_{35}
U-A	335.8	−22.1	335.6	−19.3	C-G	337.0	−20.6	335.9	−20.3
U-G	333.0	−18.0	332.1	−17.1	C-A	329.5	−16.8	330.1	−17.5
U-T	332.6	−17.4	332.8	−18.2	C-T	328.8	−16.9	329.3	−17.4
U-C	332.1	−17.3	331.6	−17.5	C-C	326.5	−15.1	326.3	−15.2
	C-probe		2′-OMe C-probe			U-probe		2′-OMe U-probe	
	T_m	ΔG_{35}	T_m	ΔG_{35}		T_m	ΔG_{35}	T_m	ΔG_{35}
C-G	338.2	−21.5	338.3	−22.0	U-A	334.9	−19.3	335.2	−20.7
C-A	332.8	−19.6	333.3	−20.2	U-G	332.4	−18.5	331.8	−19.2
C-T	332.7	−19.2	332.4	−19.6	U-T	331.0	−18.0	330.7	−18.8
C-C	332.1	−18.1	332.3	−21.0	U-C	326.9	−14.4	327.5	−16.8

[a] T_m and ΔG values are given in K and kcal/mol, respectively. Thermodynamic parameters were obtained by direct fitting of the differential melting cuves (*1*); fitting error: $T_m = \pm 0.3$ K, $\Delta H_{vH} = \pm 10\%$, $\Delta G_{35} = \pm 5\%$.

For completeness, we extended these studies to include all possible mismatches in both the ASA and FV sequence contexts. Thus, using the ASA U-probe, we also attempted to detect U-T and U-C mismatches. Substitution of the 2′-aminouridine nucleotide with a 2′-aminocytidine nucleotide (ASA C-probe, Scheme 1) allowed us to evaluate the ability of 2′-amine acylation to discriminate both C-G and U-A base pairs from the six possible mismatches in the ASA sequence context. Similarly, all possible duplexes containing either 2′-aminocytidine or 2′-aminouridine FV probes were tested in this second sequence context. For both the ASA and FV sequences, acylation was evaluated for 2′-amine-substituted probe strands directed against both DNA and RNA targets (Figure 1B).

The ASA and FV oligonucleotide model systems were selected both for their importance to human disease and also because they represent distinctive base compositions. The ASA U- and C-probes are purine-rich while the FV probe sequences are pyrimidine-rich (Scheme 1). This difference has the potential to affect selective acylation for DNA−RNA heteroduplexes, where sequence composition is known to play a fundamental role in the structure of the helix (*7*−*10*).

2′-Amine Acylation Experiments Are Performed under Nonstringent Conditions. The stability of the DNA duplexes was determined in thermal melting experiments under our standard acylation reaction conditions (10% DMSO, 0.5 M NaCl, and 100 mM Hepes, pH 8.0). Melting temperatures for all duplexes fall between 53 and 65 °C with mismatch-containing duplexes melting 2.5−10.5 °C lower than the corresponding perfect duplex (Table 1). Calculated free energies of formation at 35 °C, ΔG_{35}, for all perfect duplexes were approximately −20 kcal/mol. Depending on the sequence context and the mismatch, mismatch-containing duplexes were 1−8 kcal/mol less stable than the perfect duplex (Table 1). Large variation in duplex stability as a function of sequence is typically the case and is a major

Table 2: Thermodynamic Contributions of the DMSO Solvent and 2′-Amine Substitution[a]

		ΔΔG$_{35}$ (kcal/mol)				
		C-G	C-A	C-T	C-C	<ΔΔG>[b]
Δ DMSO	- 2′-NH$_2$	0.9	-	0.8	1	1.2 +/- 0.3
	+ 2′-NH$_2$	1.2	1.5	1.5	1.4	
Δ 2′-NH$_2$	- 10% DMSO	1.5	0.4	1	-0.1	C-G duplex, 1.4 +/- 0.2
	+ 10% DMSO	1.2	-	0.3	-0.5	Mismatch, 0.2 +/- 0.6

[a] Values were determined using FV sequences. [b] Limits on ΔΔ*G* are calculated as the standard deviation of individual ΔΔ*G*$_{35}$ values.

Table 3: Thermodynamic Contribution of the 2′-O-Me Group[a]

		ΔΔG$_{35}$ (kcal/mol)				
		N-G	N-A	N-T/U	N-C	<ΔΔG>[b]
DNA-DNA	FV C	0.3	-0.7	-0.5	-0.1	-0.9 +/- 0.8
	FV U	-0.7	-1.4	-0.8	-2.4	
	ASA C	-0.5	-0.6	-0.4	-2.9	
DNA-RNA	FV C	-2.4	-3.1	-	-	FV = -2.8 +/- 1.4
	ASA U	-0.4	-0.2	-	-	ASA = -0.3 +/- 1.1

[a] Probes contain a 2′-NH$_2$ nucleotide; experiments were performed at 10% DMSO and 0.5 M NaCl. Underlined nucleotides indicate canonical base pairs. [b] Limits for ΔΔ*G* were calculated as the mean individual fitting error.

contributor to the difficulty in using allele-specific hybridization in scoring SNPs without using additional measures such as chemical proofreading or multiple hybridization (tiling) approaches (*11*). Thermodynamic parameters were also determined for selected DNA−RNA heteroduplexes (Table 3). Perfectly paired DNA−RNA duplexes and all FV- and ASA-mismatched duplexes have T_m's of 66 °C or above, as expected (*12*−*14*).

At temperatures 10−15 °C below T_m, there is no appreciable melting or fraying for perfectly paired and mismatch-containing duplexes for either DNA−DNA or DNA−RNA duplexes. Therefore, our standard reaction temperature of 35 °C represents a nonstringent condition where all duplexes are thermodynamically indistinguishable by hybridization alone.

Thermodynamic Correction Factors for Nucleic Acid Duplexes under 2′-Amine Acylation Conditions. It is currently possible to predict with reasonable accuracy (±10% in ΔG_{35}) the T_m and ΔG_{35} for most DNA duplexes using experimentally derived parameters based on a dinucleotide model (*13*, *15*). Our experiments were performed under reaction conditions (10% DMSO and 0.5 M NaCl) and using backbone modifications (2′-NH$_2$ and 2′-O-Me) that differ from the standard conditions used to determine energies of formation for DNA duplexes. Therefore, to facilitate future calculation of ΔG_{35} values for any probe−target duplex under 2′-amine acylation conditions, we determined free energy correction values for (i) 10% DMSO solvent, (ii) the 2′-amine substitution, and (iii) the additional 2′-O-Me substitution (Tables 2 and 3).

Addition of 10% DMSO to the solvent destabilizes duplex formation by 1.2 ± 0.3 kcal/mol for both all-deoxy- and 2′-amine-substituted duplexes in the FV sequence context. Both perfect and mismatch-containing duplexes are similarly destabilized by this solvent (Table 2, rows 1 and 2). Incorporation of a single 2′-amine group destabilizes the FV duplex by 1.4 ± 0.2 kcal/mol, in good agreement with a value of 1.2 kcal/mol reported previously in a different sequence context (*16*). The 2′-amine substitution is much less destabilizing when incorporated at nucleotides forming a mismatch (ΔΔG_{35} = 0.2 ± 0.6) and may be slightly stabilizing for C-C mismatches (Table 2, rows 3 and 4).

The free energy increment for incorporating a 2′-O-Me group adjacent to the 2′-amine at position 10 for both the FV and ASA systems is highly variable (Table 3). For DNA−DNA duplexes, introduction of a 2′-O-Me nucleotide stabilizes most duplexes (ΔΔG_{35} = −0.9 ± 0.8). For DNA−RNA duplexes, introduction of a 2′-O-Me nucleotide is strongly stabilizing in the FV sequence context (ΔΔG_{35} = −2.8 ± 1.4) but just barely stabilizing, on average, for the ASA sequence (ΔΔG_{35} = −0.3 ± 1.1). In all cases, there is substantial context dependence on the contribution of the 2′-O-Me substitution to duplex stability, as evidenced by the large standard deviation in our consensus correction values (Tables 2 and 3).

In sum, we attribute a destabilization of 1.2 ± 0.3 kcal/mol to the 10% DMSO solvent. Introduction of a 2′-amine-substituted nucleotide destabilizes perfect duplexes by 1.4 ± 0.2 kcal/mol and mismatched duplexes by a small increment averaging 0.2 ± 0.6 kcal/mol. Introduction of a 2′-O-Me group at position 9 stabilizes the DNA−DNA duplexes by −0.9 ± 0.8 kcal/mol and the DNA−RNA FV and ASA sequences by −2.8 ± 1.4 and −0.3 ± 1.1 kcal/mol, respectively.

Δ*G* values were calculated for each of the duplexes using nearest-neighbor thermodynamics (ΔG_{NN}) (*6*, *15*, *17*, *18*). ΔG_{NN} values were adjusted for the presence of DMSO, for incorporation of a 2′-amino and 2′-OMe nucleotide (using consensus values reported in the previous paragraph), and for a uridine nucleotide in a DNA strand [−0.2 kcal/mol (*19*)]. Use of these correction factors improved agreement with ΔG_{35} obtained from our experimental data. Agreement averaged 10% or better, consistent with the known accuracy for these types of calculations.

2′-Amine Acylation Detects Mismatches. Acylation of the 2′-amine-containing ASA probe was initiated by the addition of excess succinimidyl ester and quenched by addition of dithiothreitol (DTT). Representative experiments performed with the ASA C-probe (Scheme 1) are shown in Figure 2. Using the C-probe, the ASA mutant allele forms a C-G pair, whereas the normal allele forms a C-A mismatch. Upon acylation, the 2′-amide product is detected as a slowly migrating species in a denaturing acrylamide gel (Figure 2A). The conformationally flexible single-stranded ASA C-probe reacts rapidly with a $t_{1/2}$ of 2 min (at 75 mM reagent). Reaction is selective for the 2′-amine group because a similar ASA C-probe lacking the 2′-amine substitution is unreactive (see all 2′-H lanes, Figure 2A).

When the 2′-amine group is constrained to form a canonical C-G base pair in a completely paired DNA−DNA duplex, the 2′-amine group is unreactive ($t_{1/2}$ = 130 min; see Figure 2A,C). The fraction of acylated ASA C-probe was calculated for each time point, and best-fit curves for the single-stranded probe, the perfect C-G duplex, and all three possible mismatched (C-A, C-T, C-C) DNA−DNA duplexes are shown in Figure 2C. The more flexible C-A, C-T, and C-C mismatches all react relatively rapidly, 28-, 14-, and 26-fold faster than the perfect C-G base pair, respectively (compare open diamonds, triangles, and inverted triangles to closed squares, Figure 2C).

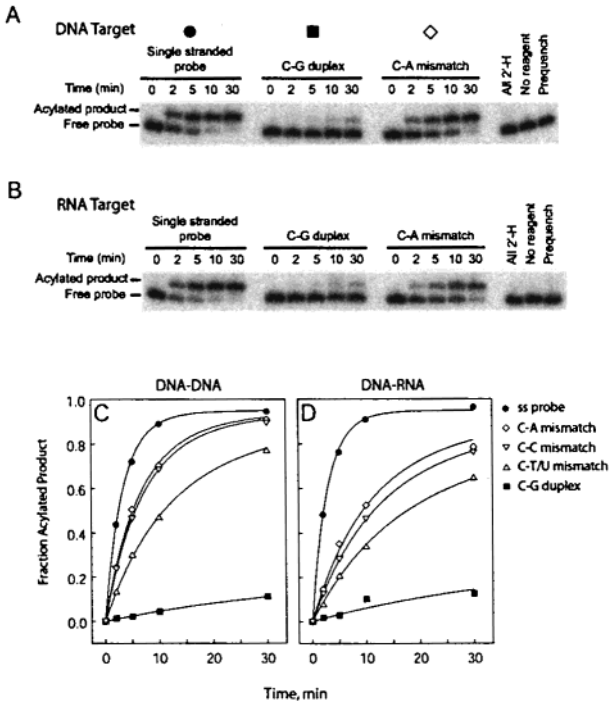

FIGURE 2: Mismatch-sensitive acylation experiments using the ASA C-probe. 2′-Amide products for reaction of the ASA C-probe directed against DNA (A) and RNA (B) targets were resolved by denaturing gel electrophoresis. The "All 2′-H" and "Prequench" lanes indicate reactions peformed with a probe oligonucleotide lacking the 2′-amine-substituted nucleotide or in which DTT was added prior to the succinimidyl ester, respectively. Acylation rates for DNA−DNA (C) or DNA−RNA (D) duplexes were determined from best-fits to eq 4.

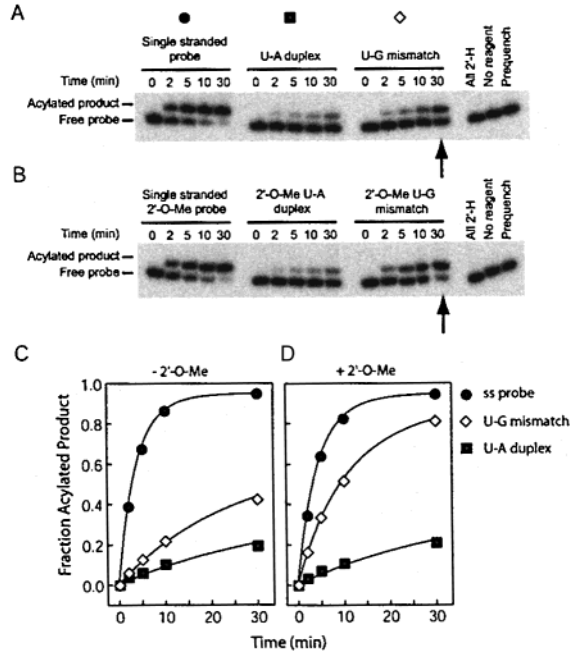

FIGURE 3: Enhanced detection of mismatches in ASA DNA−DNA duplexes for probes incorporating a 2′-O-Me group. Selective acylation experiments were performed using either the ASA U-probe (A) or the ASA 2′-O-Me U-probe (B) and monitored by denaturing electrophoresis. Arrows emphasize specific enhanced acylation for the U-G mismatch upon incorporation of the 2′-O-Me group. Kinetic analysis of 2′-amine acylation performed with the DNA ASA U-probe without (C) and with (D) a 2′-O-Me nucleotide.

Analogous experiments were performed with the ASA C-probe annealed to RNA target strands (Figure 2B). Acylation rates at the 2′-amine-substituted nucleotide in DNA−RNA heteroduplexes show the same sensitivity to base pairing as do the DNA−DNA duplexes although the absolute magnitude of kinetic discrimination is less. The C-A, C-U, and C-C mismatch-containing duplexes react with the ester 7−12-fold faster than the completely paired C-G duplex (compare open symbols with closed squares, Figure 2D).

Thus, a 2′-aminocytidine nucleotide can be used to score base pair mismatches in the ASA system in both DNA and DNA−RNA duplexes. Using the standard conditions of 35 °C and 0.5 M NaCl, we reexamined [see ref (*1*)] the selectivity of 2′-amine acylation for FV sequences (see Scheme 1) using a 2′-aminocytidine nucleotide. Discrimination between the perfect and all mismatched base pairs in the FV system was 5−14-fold in the DNA−DNA context and 6−12-fold in the DNA−RNA context. Thus, C-A, C-T/U, and C-C mismatches are robustly detected by 2′-amine acylation in both ASA and FV sequence contexts.

Poor Discrimination at 2′-Aminouridine Nucleotides. We also examined differentiating the normal ASA allele from all possible alternate sequences using a 2′-aminouridine-containing probe (see Scheme 1). Using the ASA U-probe, acylation rates were determined for the single stranded U-probe, the U-A perfect duplex, and the U-G mismatch-containing duplex (Figure 3A). Despite multiple attempts to optimize reaction conditions, it was not possible to achieve good discrimination between the U-A and U-G base pairs using 2′-amine acylation (compare the 30 min time points for reaction of the U-A duplex and U-G mismatch, Figure 3A,C). That a 2′-amino U nucleotide paired with a G is relatively unreactive is consistent with the observation that U-G mismatches are approximately as thermodynamically stable as U-A base pairs (*20*, *21*).

We explored several approaches for preferentially stabilizing the U-A base pair. Tetramethylammonium salts can increase the stability of U-A base pairs to be equal to that of C-G base pairs (*22*, *23*), and 2,6-diaminopurine is an analogue of adenine that can form three hydrogen bonds with uracil. Neither of these experimental changes increased the kinetic discrimination for 2′-amine acylation between the U-A and U-G (or U-2,6-diaminopurine) base pairs (data not shown).

Incorporation of a 2′-O-Me Group Selectively Increases the Reactivity of an Adjacent 2′-Amine Group at Mismatched Nucleotides in DNA Duplexes. As selective acylation is dependent, in large part, on local nucleotide flexibility, we investigated the possibility that introducing a small structural perturbation adjacent to the 2′-amine-substituted nucleotide might increase discrimination by 2′-amine acylation. A 2′-O-Me group was incorporated into the ASA probe oligonucleotide 5′ to the 2′-aminouridine (Figure 1B). Acylation of the flexible single stranded U-probe is efficient ($t_{1/2} = 3$ min; Figure 3A) and does not change with the incorporation of a 2′-O-Me group (Figure 3B). Incorporation of the 2′-O-Me group also does not increase the reactivity of a 2′-amine-substituted nucleotide involved in a canonical U-A base pair (compare $t_{1/2} = 63$ min in Figure 3A with a $t_{1/2} = 59$ min in Figure 3B). In contrast, introduction of a 2′-O-Me group increases the rate of acylation of the U-G base pair 3-fold (compare the 30 min time points, emphasized with arrows,

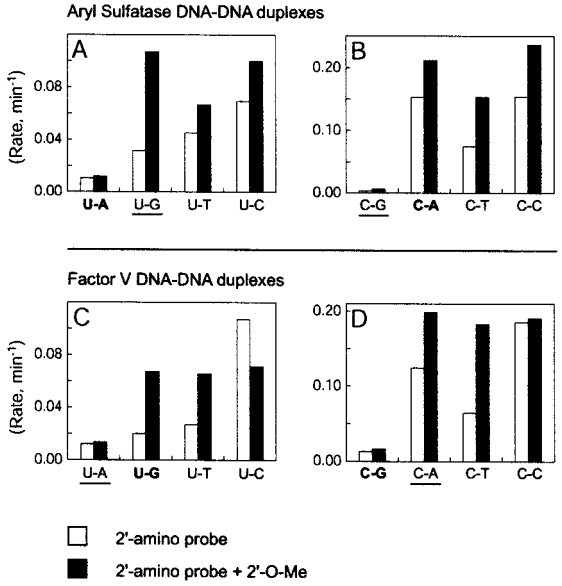

FIGURE 4: An adjacent 2′-O-Me group selectively increases 2′-amine acylation at mismatches in DNA−DNA duplexes. Open and solid bars indicate experiments performed using probes lacking or including the 2′-O-Me group, respectively. Wild-type FV or ASA alleles are in boldface, and predominant mutant alleles are underlined.

in Figure 3A,B). With incorporation of the 2′-O-Me group, the mismatched U-G base pair reacts 9-fold more rapidly than the U-A base pair. Without the 2′-O-Me group, it is difficult to discriminate robustly between the U-A and U-G base pairs as there exists only a 3-fold difference in acylation rates (Figure 3C).

ASA U-probes were also tested that either incorporated a single 2′-O-Me group 3′ to the 2′-amine group or contained two 2′-O-Me groups, one on each side of the 2′-amino nucleotide. Both test probes showed a specific increase in the rate of acylation for 2′-amine groups involved in a mismatched U-G base pair as compared to a U-A base pair. By directly comparing the acylation rates of these three different 2′-O-Me probes, we found that the 2′-O-Me group has the largest effect on acylation rates when placed 5′ to the 2′-amine group (data not shown).

Variants of the ASA and FV DNA C- and U-probes were each synthesized incorporating a 2′-O-Me group 5′ to the 2′-aminouridine or -cytidine nucleotide (Figure 1B). These probes were annealed to DNA targets, and 2′-amine pseudo-first-order acylation reactions were followed for the canonical base pairs and all possible mismatches. We calculated acylation rates for each duplex (for example, see Figure 3C), and the effect of introducing the 2′-O-Me group is summarized in Figure 4.

Introduction of a 2′-O-Me group adjacent to the 2′-amino nucleotide has a systematic effect for DNA probe−DNA target duplexes [compare open (no 2′-O-Me) with closed (+2′-O-Me) bars in Figure 4]. For all of the ASA-based sequences, incorporation of the 2′-O-Me group increased the rate of 2′-amine acylation for the mismatched duplexes without a significant concomitant increase in the reaction of the perfect duplex (compare closed and open bars in Figure 4A,B). Thus, kinetic discrimination was enhanced in all cases.

Analogous experiments were performed with the FV U- and C-probes (Figure 4C and 4D, respectively). Incorporation of a single 2′-O-Me group 5′ to the 2′-amine group also did not change significantly the rate of acylation for the C-G or U-A perfect duplexes in the FV system. Instead, incorporation of the 2′-O-Me group specifically and consistently increases the reactivity of the mismatched nucleotides in a DNA−DNA based duplex. For example, the least reactive C-T mismatch-containing duplex becomes acylated at least 11-fold faster than the perfect C-G duplex. This improves on the 5-fold rate discrimination seen between the C-T mismatch duplex and the C-G perfect duplex without the 2′-O-Me group (Figure 4D). The 2′-amine FV U-G and U-T mismatch-containing duplexes show a significant increase in the rate of acylation upon incorporation of a 2′-O-Me group, such that analytical discrimination between mismatches and perfect base pairs becomes possible (Figure 4C). There is some sequence variation in the contribution of the 2′-O-Me group because the acylation rate of the FV 2′-O-Me U-probe−C mismatched duplex decreases relative to a duplex lacking the 2′-O-Me group but still reacts at least 5-fold faster than the perfect U-A duplex.

2′-O-Me Groups Decrease Acylation Selectivity in DNA−RNA Hybrid Duplexes. As described above, probes containing 2′-aminocytidine nucleotides (lacking the 2′-O-Me moiety) showed good kinetic discrimination between the perfect and mismatched duplexes for DNA−RNA heteroduplexes in both ASA and FV sequence contexts: mismatched duplexes in both systems reacted 6−12-fold more rapidly than the perfect duplexes. However, using probes containing 2′-aminouridine did not yield good discrimination between perfect and mismatched probe−RNA heteroduplexes (see Figure 5A). We then tested whether incorporation of a 2′-O-Me group into a DNA−RNA duplex would selectively increase the rate of acylation in mismatched heteroduplexes, as occurs for DNA−DNA duplexes.

We formed heteroduplexes between the ASA U- and ASA 2′-O-Me DNA U-probes and RNA target strands, subjected the duplexes to 2′-amine acylation, and calculated reaction rates (Figure 5A,B). The flexible single stranded DNA probes react rapidly as expected (closed circles in Figure 5A,B). However, it is not possible to discriminate between the perfect U-A duplex and mismatched duplexes with either probe because all the mismatch-containing duplexes were relatively unreactive (compare open symbols with closed squares in Figure 5A,B). In fact, for both ASA U- and ASA 2′-O-Me U-probes, the mismatched U-G base pair is less reactive than the canonical U-A pair. Upon incorporation of the 2′-O-Me group, discrimination between duplexes becomes worse [compare ASA U-probe (open bars) with 2′-O-Me ASA U-probe (closed bars) in Figure 5C].

Similar experiments, analyzing the effects of 2′-O-Me incorporation, were performed using the ASA C-probe hybridized to target RNA (Figure 5D). Whereas it is possible to discriminate between mismatches and perfect base pairs across from a 2′-aminocytidine nucleotide in this heteroduplex system, the introduction of a 2′-O-Me group reproducibly decreases 2′-amine acylation rates in all duplexes (compare open and closed bars, Figure 5D).

Comparable experiments were also carried out incorporating a 2′-O-Me group into C- and U-probes for DNA−RNA heteroduplexes in the FV sequence context. As for ASA sequences, incorporation of a 2′-O-Me group both decreases overall reaction rates and also decreases kinetic discrimina-

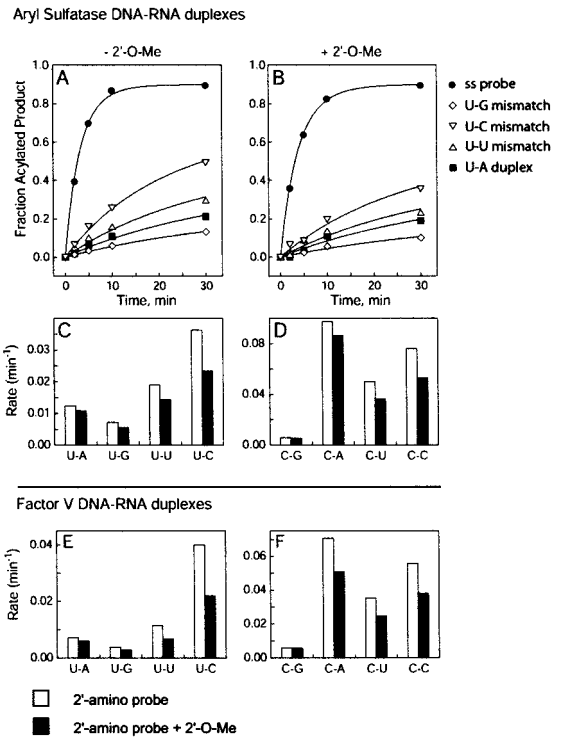

FIGURE 5: Introduction of an adjacent 2′-O-Me group decreases kinetic discrimination by 2′-amine acylation for DNA−RNA heteroduplexes. Kinetic profiles for mismatch-dependent acylation in DNA−RNA duplexes incorporating either the ASA U-probe (A) or the ASA 2′-O-Me U-probe (B). Data from panels A and B are compared directly for the ASA U-probe in panel C. Open and closed bars indicate pseudo-first-order acylation rates obtained in the absence and presence of the 2′-O-Me group, respectively. A systematic study of DNA−RNA heteroduplexes shows that incorporation of a 5′ 2′-O-Me group into the ASA U-probe (C), ASA C-probe (D), FV U-probe (E), and FV C-probe (F) decreases the rate of 2′-amine acylation in all cases.

tion between canonically paired and mismatch-containing duplexes (compare open and closed bars in Figure 5E,F).

Thus, incorporation of a 2′-O-Me nucleotide in both the FV and ASA DNA probe strands invariably decreases the discrimination between the mismatched and perfect heteroduplexes at RNA target strands. It is therefore possible to score reliably mismatches at RNA targets across from a 2′-amine-substituted cytidine nucleotide (without the additional 2′-O-Me modification, see Figure 5D,F) but not across from a 2′-aminouridine nucleotide.

DISCUSSION

Detection of Mismatches, SNPs, and RNA Hybridization by Selective 2′-Amine Acylation. In this work, we systematically explored the ability of 2′-amine acylation to interrogate the base paired state of 2′-amine-substituted cytidine and uridine nucleotides in DNA−DNA and DNA−RNA duplexes. We sought to optimize an initial finding (*1*) that 2′-amine-substituted nucleotides that form canonical base pairs are relatively resistant to acylation at the 2′-amine group as compared with unconstrained or mismatch-forming nucleotides (see Figure 1A). In all cases, discrimination by 2′-amine acylation was evaluated under nonstringent hybridization conditions, at least 10 °C below duplex melting temperatures.

2′-Amine acylation represents a robust approach for tagging selectively mismatches in DNA−DNA homoduplexes. Strikingly, incorporation of a 2′-O-Me group 5′ to the unique 2′-amino nucleotide universally yields enhanced discrimination between perfect and mismatch-containing DNA−DNA duplexes. Using 2′-amino and 2′-O-Me dual-substituted probes (Figure 1B), discrimination between C-G and U-A base pairs and all possible mismatches is good. 2′-Aminocytidine and -uridine nucleotides involved in mismatched base pairs are acylated 5−35-fold faster than the corresponding canonical base pairs (Figure 4). Detection of mismatches at 2′-aminopyrimidine residues was demonstrated for two sequence contexts under a single nonstringent temperature.

Mismatches are also robustly detected as rapid acylation for RNA target strands across from 2′-amine-substituted cytidine nucleotides but not across from 2′-aminouridine nucleotides (Figure 5). Discrimination is 6−17-fold, depending on the sequence context. Thus, 2′-amine acylation can be used to detect SNPs directly in RNA targets across from C residues and to quantify RNA hybridization for any sequence containing an internal guanosine residue.

Model for Preferential Local Destabilization of Mismatches by Incorporation of a 2′-O-Me Group in DNA−DNA but Not in DNA−RNA Heteroduplexes. Addition of a 2′-O-Me group adjacent to the 2′-amine group selectively increases the acylation rate for 2′-amino nucleotides involved in mismatched base pairs in DNA−DNA duplexes (compare open and closed bars, Figure 4). Because the 2′-O-Me group does not affect acylation of 2′-amine groups involved in canonical base pairs, this modification functions to maximize kinetic discrimination between canonical and mismatched base pairs. This contribution by the 2′-O-Me group is most clearly illustrated by discrimination between U-A and U-G base pairs in both the FV and ASA sequence contexts. A single 2′-O-Me group introduces a structural perturbation that specifically increases the local flexibility at the site of the U-G mismatch to yield robust discrimination between completely paired and mismatch-containing duplexes (compare open and closed bars in Figure 4A,C).

In the context of 2′-amine C-probes, where discrimination is good in the absence of any additional modification, the introduction of a 2′-O-Me group improves kinetic discrimination in the DNA−DNA duplexes to at least 23-fold in the ASA system and to at least 11-fold in the FV system (compare open and closed bars in Figure 4B,D).

In contrast, in a DNA−RNA heteroduplex, incorporating a 2′-O-Me group decreases the efficiency of 2′-amine acylation at mismatched nucleotides (Figure 5). Thus, the proximal 2′-O-Me group has dramatically different consequences depending on global duplex structure. 2′-Amine acylation is selectively enhanced at mismatches in B-form DNA−DNA duplexes, but is suppressed in A-like (*24*−*27*) DNA−RNA heteroduplexes.

Structurally, electronegative groups at the 2′-ribose position, such as an O-Me group, favor the ribose C3′-endo conformation (*28*−*30*). The 2′-O-Me nucleotide thus approximates an RNA-like A-form conformation. This conformation is stabilized by intra- and intermolecular hydrogen bonding interactions and distinct patterns of hydration (*25*). The structural bias toward an A-form conformation can propagate into adjacent nucleotides, as single 2′-O-Me groups incorporated into DNA strands have been shown to nucleate a local A-type conformation (*24*−*27*). The enhanced reactiv-

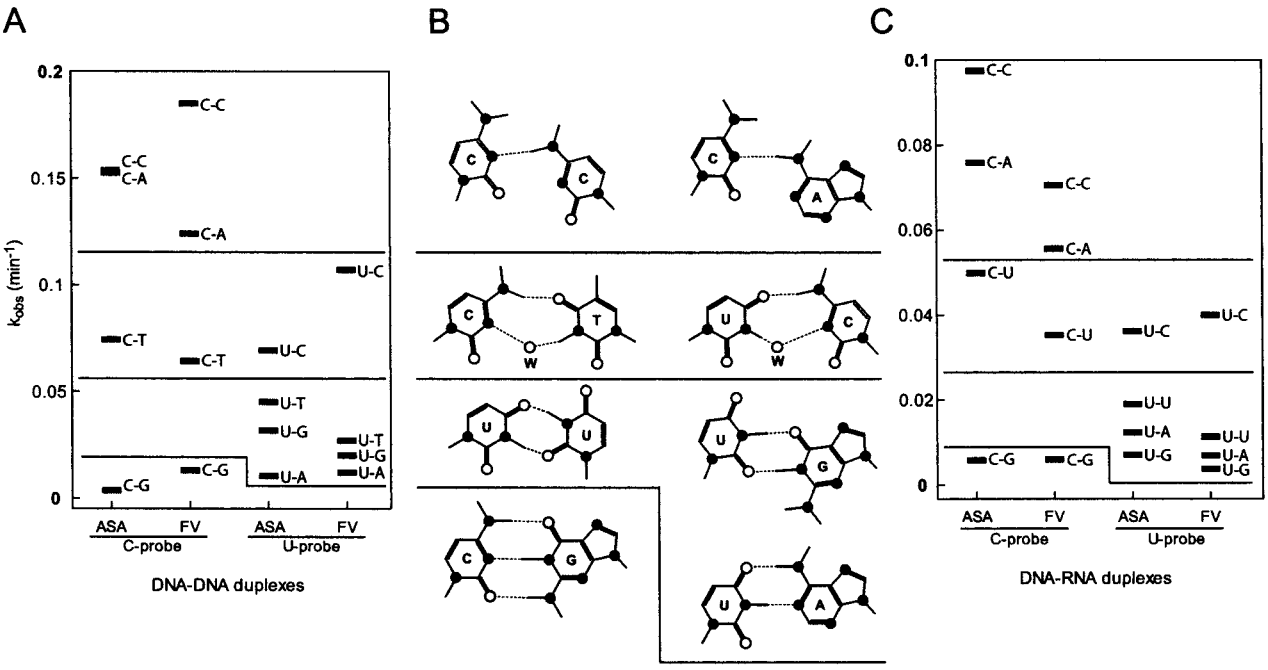

FIGURE 6: Correlation between 2′-amine acylation and the number and strength of nucleobase hydrogen bonds. Psuedo-first-order 2′-amine acylation rates for the perfect (C-G and U-A) base pairs and mismatched (C-A, C-T/U, C-C, U-G, U-T/U, U-C) base pairs are compared for DNA−DNA (A) and DNA−RNA (C) duplexes. (B) Base pair and mismatch structures (*31*−*39*). Nitrogen and oxygen atoms are shown as filled and open circles, respectively. W indicates crystallographically defined water molecules. Base pairs containing cytidine are derived from DNA−DNA crystal structures and are expected to be similar in DNA−RNA heteroduplexes. Uridine-containing base pairs are derived from RNA−RNA crystal structures.

ity of 2′-amine groups in DNA−DNA duplexes that also contain a 2′-O-Me is consistent with local destabilization of the B-form duplex by a segment of A-like structure.

Just the opposite is true for DNA−RNA heteroduplexes, which have substantial A-like character. Introducing a RNA-like 2′-O-Me nucleotide into the DNA probe strand is expected to stabilize locally a more A-form conformation (*24*−*26*). Adjacent base pairs would experience less local flexibility which we observe as a slower 2′-amine acylation rate.

The Hydrogen Bonding Pattern of Base Pairs Is Correlated to the Rate of Acylation. Trends in relative 2′-amine acylation reactivities for canonical U-A and C-G base pairs and for the mismatched base pairs are essentially identical for both ASA and FV sequence contexts (Figure 6A). This trend in relative reactivity is preserved both for DNA−DNA and for DNA−RNA duplexes (Figure 6C), despite the fact that local helix geometries are significantly different for these duplexes.

For the 2′-amino C-probe series, the reactivity trend is C-C > C-A > C-(T/U) > C-G. For U-probes, reactivity is U-C > U-(T/U) > U-G ∼ U-A. Strikingly, for both C- and U-probes, the trend in 2′-amine acylation reactivity shows a good correlation with the strength of hydrogen bonding in each pair (Figure 6B).

Structural studies indicate that C-A and C-C mismatches form a single hydrogen bond at neutral pH (*31*−*33*). In contrast, C-T base pairs are stabilized by two hydrogen bonds, one of which is water-mediated (*32*, *34*). The C-T mismatch is constrained by an additional water-mediated hydrogen bond and is, correspondingly, acylated at a slower rate than the more flexible C-A and C-C mismatches. The unreactive C-G base pair is the most highly constrained with three stabilizing hydrogen bonds (see Figure 6B).

A similar relationship between 2′-amine acylation and hydrogen bonding also holds for reaction at uridine nucleotides. A U-C mismatch forms one direct hydrogen bond and a second water-mediated hydrogen bond [Figure 6B; (*35*)]. Thus, both the U-C and C-(T/U) pairs are stabilized by one direct and one water-mediated hydrogen bond and are observed to be less reactive than mismatches stabilized by a single hydrogen bond. Both U-A pairs and U-G mismatches form two stable hydrogen bonds (*35*, *36*) and are unreactive (in the absence of the perturbing 2′-O-Me group). U-T base pairs can also form two hydrogen bonds, although with a substantially altered helix geometry (*37*−*39*). Each base pair that forms two hydrogen bonds (U-A, U-G, and U-T/U) is characterized by a similar acylation rate that is slower than for the U-C base pair (Figure 6).

There appears to be a structural threshold for efficient 2′-amine acylation. All nucleotide pairs that form two or more hydrogen bonds are relatively unreactive (Figure 6), and the addition of a third hydrogen bond (for C-G pairs) does not further reduce reaction at 2′-amine groups. The strong overall correlation between local hydrogen bonding and 2′-amine acylation, for reactions performed under conditions where duplexes and mismatches are not thermodynamically distinguishable (10−15 °C below T_m), provides strong support for the original proposal (*2*) that 2′-amine acylation reports local nucleotide flexibility.

Future Prospects. 2′-Amine acylation represents a robust approach for interrogating nucleic acid mismatches and for quantifying RNA hybridization. The selective tagging chemistry exploits the inherent flexibility of a mismatched or unpaired nucleotide to distinguish it from a canonically paired nucleotide. This chemistry potentially represents a significant advantage over existing allele-specific hybridization methods for scoring SNPs and quantifying RNA levels as 2′-amine

acylation predominantly reports local nucleotide structure. Successful mutation detection under a single reaction condition is generalizable to diverse sequence contexts, at both 2′-amine-substituted uridine and cytidine nucleotides in DNA duplexes. Mismatch detection in DNA−RNA hybrid duplexes is also possible across from 2′-aminocytidine nucleotides.

We envision several applications for interrogation of mismatches by 2′-amine acylation. Selective 2′-amine acylation coupled with high throughput hybridization techniques would provide an additional level of selectivity for scoring single base changes in amplified DNAs without the requirement for time-consuming optimization steps. Second, sequence variation in RNA could be scored directly, potentially without prior amplification. Finally, since formation of probe−RNA hybrids dramatically decreases reactivity at 2′-amine-substituted cytidine nucleotides (Figure 5D,F), selective acylation represents a promising approach for quantifying absolute amounts of RNA.

ACKNOWLEDGMENT

We thank the Macromolecular Interactions Facility at the University of North Carolina at Chapel Hill for use of the temperature-controlled CD spectrometer and C. Scott Phelps for helpful discussions on 2′-O-Me experiments.

REFERENCES

1. John, D. M., and Weeks, K. M. (2000) *Chem. Biol. 7*, 405−410.
2. Chamberlin, S. I., and Weeks, K. M. (2000) *J. Am. Chem. Soc. 122*, 216−224.
3. Stein, C., Gieselmann, V., Kreysing, J., Schmidt, B., Pohlmann, R., Waheed, A., Meyer, H. E., O'Brien, J. S., and von Figura, K. (1989) *J. Biol. Chem. 264*, 1252−1259.
4. Bertina, R. M., Koeleman, B. P. C., Koster, T., Rosendaal, F. R., Dirven, R. J., de Ronde, H., van der Velden, P. A., and Reitsma, P. H. (1994) *Nature 369*, 64−67.
5. Gralla, J., and Crothers, D. M. (1973) *J. Mol. Biol. 78*, 301−319.
6. Santa Lucia, J., Jr. (1998) *Proc. Natl. Acad. Sci. U.S.A. 95*, 1460−1465.
7. Salazar, M., Fedoroff, O. Y., Miller, J. M., Ribeiro, N. S., and Reid, B. R. (1993) *Biochemistry 32*, 4207−4215.
8. Lesnik, E. A., and Freier, S. M. (1995) *Biochemistry 34*, 10807−10815.
9. Gyi, J. I., Conn, G. L., Lane, A. N., and Brown, T. (1996) *Biochemistry 35*, 12538−12548.
10. Gyi, J. I., Lane, A. N., Conn, G. L., and Brown, T. (1998) *Biochemistry 37*, 73−80.
11. Shi, M. M. (2001) *Clin. Chem. 47*, 164−172.
12. Sugimoto, N., Nakano, S., Katoh, M., Matsumura, A., Nakamuta, H., Ohmichi, T., Yoneyama, M., and Sasaki, M. (1995) *Biochemistry 34*, 11211−11216.
13. Peyret, N., and Santa Lucia, J., Jr. HyTher program. http://ozone.chem.wayne.edu/Hyther/hythermenu.html.
14. Sugimoto, N., Nakano, M., and Nakano, S. (2000) *Biochemistry 39*, 11270−11281.
15. Santa Lucia, J., Jr., Allawi, H. T., and Seneviratne, P. A. (1996) *Biochemistry 35*, 3555−3562.
16. Aurup, H., Tuschl, T., Benseler, F., Ludwig, J., and Eckstein, F. (1994) *Nucleic Acids Res. 22*, 20−24.
17. Allawi, H. T., and Santa Lucia, J., Jr. (1998) *Biochemistry 37*, 9435−9444.
18. Allawi, H. T., and Santa Lucia, J., Jr. (1998) *Nucleic Acids Res. 26*, 2694−2701.
19. Wang, S., and Kool, E. T. (1995) *Biochemistry 34*, 4125−4132.
20. Sugimoto, N., Kierzek, R., Freier, S. M., and Turner, D. H. (1986) *Biochemistry 25*, 5755−5759.
21. He, L., Kierzek, R., Santa Lucia, J., Jr., Walter, A. E., and Turner, D. H. (1991) *Biochemistry 30*, 11124−11132.
22. Melchior, W. B., and von Hippel, P. H. (1973) *Proc. Natl. Acad. Sci. U.S.A. 70*, 298−302.
23. Nguyen, H.-K., Fournier, O., Asseline, U., Dupret, D., and Thuong, N. T. (1999) *Nucleic Acids Res. 27*, 1492−1498.
24. Lesnik, E. A., Guinosso, C. K., Kawasaki, A. M., Sasmor, H., Zounes, M., Cummins, L. L., Ecker, D. J., Cook, P. D., and Freier, S. M. (1993) *Biochemistry 32*, 7832−7838.
25. Lubini, P., Zurcher, W., and Egli, M. (1994) *Chem. Biol. 1*, 39−45.
26. Lesnik, E. A., and Freier, S. M. (1998) *Biochemistry 37*, 6991−6997.
27. Venkateswarlu, D., Lind, K. E., Mohan, V., Manoharan, M., and Ferguson, D. M. (1999) *Nucleic Acids Res. 27*, 2189−2195.
28. Uesugi, S., Miki, H., Ikehara, M., Iwahashi, H., and Kyogoku, Y. (1979) *Tetrahedron Lett.*, 4073−4076.
29. Guschlbauer, W., and Jankowski, K. (1980) *Nucleic Acids Res. 8*, 1421−33.
30. Ikehara, M. (1984) *Heterocycles 21*, 75−90.
31. Boulard, Y., Cognet, J. A. H., Gabarro-Arpa, J., Bret, M. L., Carbonnaux, C., and Fazakerley, G. V. (1995) *J. Mol. Biol. 246*, 194−208.
32. Boulard, Y., Cognet, J. A. H., and Fazakerley, G. V. (1997) *J. Mol. Biol. 268*, 331−347.
33. Peyret, N., Seneviratne, P. A., Allawi, H. T., and Santa Lucia, J., Jr. (1999) *Biochemistry 38*, 3468−3477.
34. Tanaka, Y., Kojima, C., Yamazaki, T., Kodama, T. S., Yasuno, K., Miyashita, S., Ono, A. M., Ono, A. S., Kainosho, M., and Kyogoku, Y. (2000) *Biochemistry 39*, 7074−7080.
35. Holbrook, S. R., Cheong, C., Tinoco, I., and Kim, S.-H. (1991) *Nature 353*, 579−581.
36. Chen, X., McDowell, J. A., Kierzek, P., Krugh, T. R., and Turner, D. H. (2000) *Biochemistry 39*, 8970−8982.
37. Santa Lucia, J., Jr. Kierzek, R., and Turner, D. H. (1991) *Biochemistry 30*, 8242−8251.
38. Gervais, V., Cognet, J. A. H., Bret, M. L., Sowers, L. C., and Fazakerley, G. V. (1995) *Eur. J. Biochem. 228*, 279−290.
39. Baeyens, K. J., DeBondt, H. L., and Holbrook, S. R. (1995) *Struct. Biol. 2*, 56−62.

BI025611D